Activation of Methanes by Doubly Charged Metal Dication Complexes in the Gas Phase

Joseph K Koka[1,2*], Lifu Ma[1] and Anthony J Stace[1]

[1]*School of Chemistry, University of Nottingham, University Park, Nottingham NG7 2RD, UK*

[2]*Department of Chemistry, University of Cape Coast, Ghana*

_____

ABSTRACT

A doubly charged metal dication complexes [Mn(Pyridine)4]2+ ions were formed and further activated with methane in the gas phase. [Mn(Pyridine)CH4]2+, [Mn(Pyridine)2CH4]2+, [Mn(Pyridine)3CH4]2+, [MnPy2Me2]2+ [MnPy3Me2]2+ and [Mn(Pyridine)4CH4]2+ were successfully identified after the experimental analysis. The average pyridine binding energy, calculated at the different levels of theory of zero point energy are in realistic agreement. The binding energies of methane decrease drastically with increasing number of pyridine ligands in the order of [Mn(Pyridine)CH4]2+>[Mn(Pyridine)2CH4]2+>[Mn(Pyridine)3CH4]2+> [Mn(Pyridine)4CH4]2+. The optimised structure of [Mn(Pyridine)4(CH4)]2+ indicated C1 symmetry with the methane-manganese ion distance approximately r=2.00 Å.

DFT calculated binding energy of methane with Mn2+ was 15.13 kJ/mol while the binding energy calculated on the potential energy curve (PEC) was 17.37 kJ/mol. This higher interaction energy calculated from the PEC was due to the fact that the charge +2 was assumed for the metal ion in the calculations, but at the optimised geometry the DFT calculated actual charge on the metal ion was (Z=1.43). The calculated binding energy of methane with manganese pyridine dication complex ion was drastically overestimated on the PEC by approximately 15% compare to DFT.

Keywords: Methane; Doubly charged metal dication complexes; Gas phase

_____

INTRODUCTION

Methane is the most stable, simplest and the most abundant alkane molecule. It is also one of the most ubiquitous feed stocks available in large amounts from petrological as well as biogenic resources. In addition, it is the second most important anthropogenic greenhouse gas after CO_2 [1]. Its rise in air concentration is the result of non-sustainable farming, and chemical and energy power processes. Although the amount of methane emissions is five times less than CO2, they are similarly problematic because methane can retain approximately 23 times more heat than CO2 in the atmosphere. Because of this, a large-scale chemical conversion of methane into other valuable and/or environmentally friendly chemical compounds would have a tremendous impact on the climate and, due to the low-cost of this feedstock, on the chemical industry [1-9].

The aim of this research was to form doubly charged metal dication complexes $[Mn(Pyridine)_4]^{2+}$ ions, activate them with methane in the gas phase and calculate the binding energy of methane to the metal complexes. Once methane is activated, it can serve as feedstock formation in a vast variety of prominent industrial reactions, notably synthesis gas (syngas) formation [10,11]. The syngas formation can be possible through any of the following ways namely: (a)

steam reforming [11,12,13]. $CH_4 + H_2O \rightarrow CO + 3H_2$, $\Delta fH = +206$ kJ mol^{-1} (b) dry reforming [14-19]. $CH_4 + CO_2 \rightarrow 2CO + 2H_2$ $\Delta fH^= +247$ kJ mol-1 (c) methane partial oxidation [20-23] $CH_4 + 1/2O_2 \rightarrow CO + 2H_2$ $\Delta fH^= -36$ kJmol-1.
The generated current H2/CO from the syngas could be used in Fischer–Tropsch reaction [11,24,25,26,27] to obtain long-chain hydrocarbons as detailed in equations (d) and (e). Furthermore, the generated H2 could be relevant in the application of fuel cells [28-30].
(d) $nCO + (2n+1)H_2 \rightarrow C_nH_{2n+2} + nH_2O$ $\Delta fH^= -347$ kJmol-1(n=2)
(e) $nCO + 2nH_2 \rightarrow C_nH_{2n} + nH_2O$ $\Delta fH^= -210$ kJmol-1(n=2).
On the other hand, potentially through CO2 oxidative coupling methane can be converted to ethane equation (f) and ethylene equation (g) [6,7,31,32]
(f) $2CH_4 + CO_2 \rightarrow C_2H_6 + CO + H_2O$ $\Delta fH^= +106$ kJmol-1
(g) $2CH_4 + 2CO_2 \rightarrow C_2H_4 + 2CO + 2H_2O$ $\Delta fH^= +284$ kJmol-1.
When compared with reactions taking place in the condense phase, the advantages derive from experiments performed in the gas phase activation of small molecules (methane) are: (i) reactive collisions can be controlled in terms of their frequency and energy; (ii) precise mechanisms are more easily identified and analysed using, for example, isotopes of methane CD4. Studies in gas phase can be seen as providing fundamental insight into possible low energy pathways for bond activation, and will ultimately provide a means of identification mechanisms for feedstock formation [2,3].

Experimental section

$[Mn(Pyridine)_4]^{2+}$ ions were synthesised in the gas phase and their spectra recorded via UV photofragment spectroscopy within an ion trap mass spectrometer cooled to between 100-150 K. A schematic diagram of the apparatus is shown in Figure 1. Neutral Mn[Pyridine]n clusters were generated via the pickup technique [4], whereby argon carrier gas at a pressure of 130 psi was passed through a reservoir of pyridine held at room temperature. The resultant mixture, containing approximately 1% pyridine vapour, underwent supersonic expansion through a 50mm diameter nozzle before passing through a 1 mm diameter skimmer.

The emerging beam of mixed argon/pyridine clusters then passed over the top of a Knudsen cell containing manganese chips heated to 1150°C, which was sufficient to generate a metal vapour pressure of 10^{-3} to 10^{-2} mbar. Collisions between metal vapour and the mixed clusters generated neutral metal-containing clusters, which were then ionised by high energy electron impact (100 eV) in the ion source of a quadrupole mass spectrometer (Extrel). From the mixture a doubly charged ions (Figure 2), $[Mn(Pyridine)_4]^{2+}$ was mass selected and directed by an ion guide into a Paul ion trap. The end caps of the latter were grounded and continuously cooled through direct contact with a liquid nitrogen reservoir. As a consequence, helium buffer gas (5×10^{-4} mbar) contained within the trap was also cooled and over a total trapping time of 1s, collisions between the helium and trapped ions led to a considerable reduction in the internal energy content of the latter [5]. Based on the observation of unimolecular decay by trapped ions, the internal temperature was thought to drop from 4500 K to somewhere in the range 100–150 K. This cooling procedure has led to the appearance of discrete structure in the spectra.
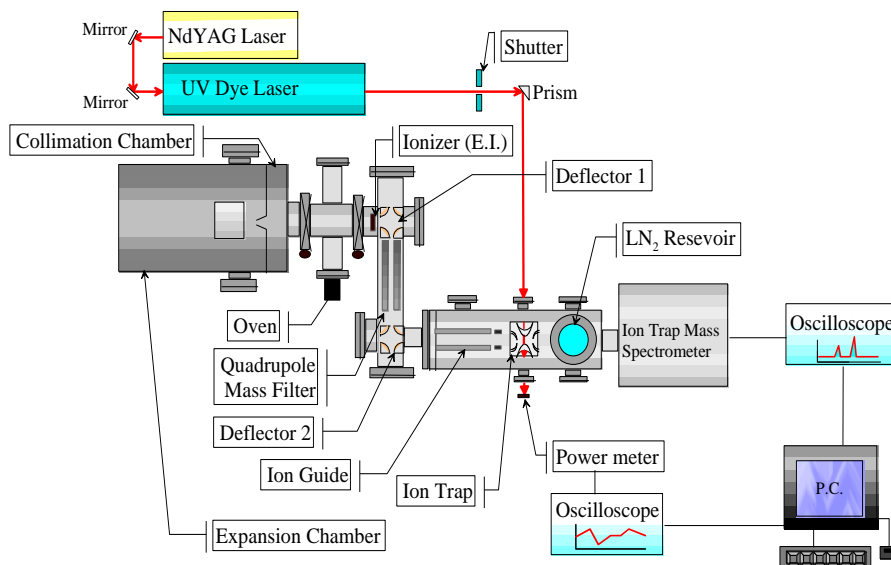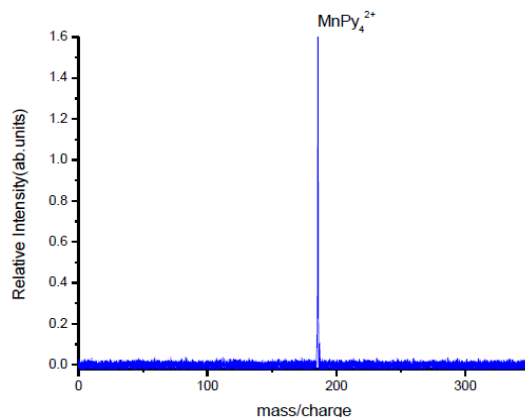

Figure 1. The diagram illustrating the experimental set up

MATERIAL AND METHODS

Figure 2. Mass spectrum of the [Mn(Pyridine)$_4$]$^{2+}$

With the introduction of methane gas into the trap a typical example of a mass spectrum is reported (Figure 3) and was produced with a mass/charge scale assigned based on the position of the parent peaks. Without energy input via the laser, metal complex ions can fragment by collision induced dissociation (CID) process probably due to the parent complex ion colliding with the helium atom which acts as a buffer gas. Two additional peaks of the parent picking up one molecule of methane at 193.5amu and a daughter cluster of [MnPy$_3$]$^{2+}$ picking one and two molecules of methane at 154 amu and 162 amu respectively were observed.
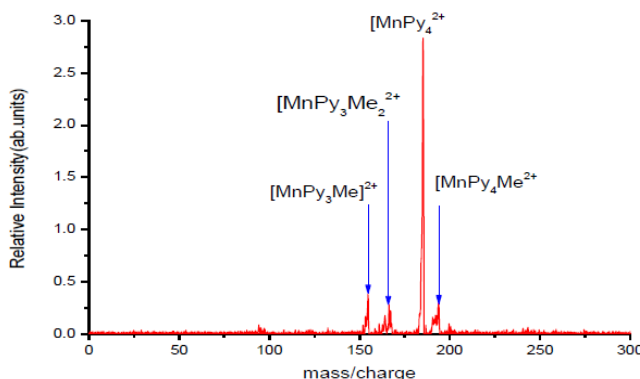
Figure 3. Mass spectrum of manganese pyridine dication complex ion when methane gas was introduced

The methane peaks are observed to have some associated splitting with smaller peaks that have a mass/charge ratio of about one point smaller corresponding to the peaks of one and two mass units lighter than the main peak. Being monoisotopic, manganese is one of 26 chemical elements which have only a single stable isotope; hence such splitting might be highly considered to be due to the isotopes of carbon and/or nitrogen within the pyridine ligands or loss of a hydrogen atom. Alternatively, considering the proportionally weak signal, electronic noise and background material could also play a major role in this kind of splitting.

Following a 300 ms collection and cooling period, the ions were irradiated with seven 10 ns pulses of tunable UV radiation from the frequency-doubled output of Nd: YAG-pumped dye laser, before being ejected for mass analysis

and signal averaging. This gave a total duty cycle of 1s for each period of ion injection and excitation. Photon absorption led to fragmentation and the intensities of the precursor and all fragment ions were monitored as a function of photon energy. The cycle of trapping and laser excitation was repeated 200 times to yield a photofragment mass spectrum at a fixed wavelength. All of the ions shown were ejected and collected during each single sweep of the RF trapping voltage, which meant that their individual intensities could be monitored simultaneously. Overall, this averaging procedure gave an excellent signal/noise ratio after activation with methane and a typical example is shown in Figure 4.

The corresponding UV photofragmentation yield plotted as a function of photon energy marked as indicated alongside at 39838.77. No hydrated cluster of the metal pyridine dication complex ion was recorded probably due to the fact that apart from cryopumping the chamber was also baked electrically to aid complete elimination of water. The mass spectra generated revealed three parent ions; $[Mn(Pyridine)_4]^{2+}$ at 185.5amu with the others picking up methane molecule(s) to form $[Mn(Pyridine)_4CH_4]^{2+}$ at 193.5amu and $[Mn(Pyridine)_4(CH_4)_2]^{2+}$ at 201.5amu. In addition doubly charged daughter ions were observed from the parent fragment losing a single pyridine with the daughter fragment peak corresponding to coordinately unsaturated $[Mn(Pyridine)_3]^{2+}$ at 146 amu, with the ability of this daughter fragment to pick up methane molecule(s) to form $[Mn(Pyridine)_3CH_4]^{2+}$ at 154 amu and $[Mn(Pyridine)_3(CH_4)_2]^{2+}$ at 162 amu. A fragmentation path of the parent fragment losing two molecules of pyridine and the resultant daughter fragment picking up methane molecule to form $[Mn(Pyridine)_2CH_4]^{2+}$ at 114.5 amu was observed. The fragment of $[MnPyridine]^+$ at 134 amu could be the result of the dissociation of $[Mn(Pyridine)_4]^{2+}$ in a charge transfer process resulting in the manganese pyridine monovalent complex ion picking two methane molecules to form $[MnPyridine(CH_4)_2]^+$ at 166 amu.

Furthermore, two additional singly charged daughter fragments namely, a protonated pyridine emanating from charge transfer processes, $PyridineH^+$, and a pyridine picking up methane molecule to form $PyridineCH_4^+$ are also observed at 80 and 95 amu respectively.
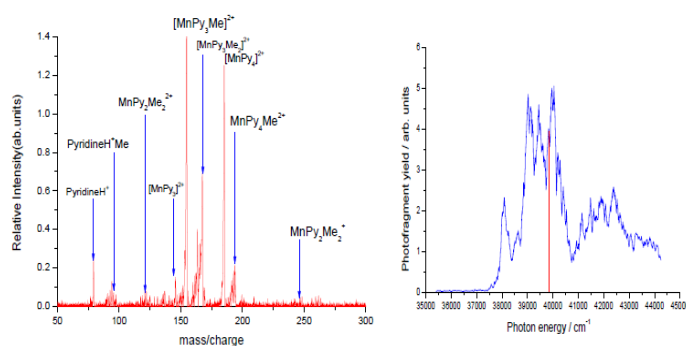

Figure 4. Photofragment mass spectrum of $[Mn(Pyridine)_4CH_4]^{2+}$ (39839 cm^{-1})

CALCULATIONS

A ground state calculation of the binding energy of methane with manganese pyridine complex dications and pyridine with Mn+2 ion were carried out at zero point energy, corrected at 298 K using Gaussian 09 using BVP86

and TPSSh with 6-311G++(d, p) basis sets. For [Mn(Pyridine)$_4$ CH$_4$]$^{2+}$ complexes, the binding energy of each methane molecule is maximised at the optimised structure where there is no imaginary frequency and the results are summarised in Table 1.

Table 1. Binding energies for the Mn2+ complexes with respect to various products formed and calculated using both BVP86/6311++G(d, p) and TPSSh/6311++G(d, p)

Reaction	BVP86/kJ/mol	TPSSh/kJ/mol
[MnPy$_4$]$^{2+}$ → Mn^{2+}+4Py	1732.44	1732.42
[MnPy$_3$]$^{2+}$ → Mn^{2+}+ 3Py	1557.01	1557.00
[MnPy$_2$]$^{2+}$ → Mn^{2+}+ 2Py	864.06	864.07
[MnPy]$^{2+}$+→ Mn^{2+}+ Py	464.84	464.84
[MnPy$_4$Me]$^{2+}$ → [MnPy$_4$]$^{2+}$ +Me	15.13	15.11
[MnPy$_3$Me]$^{2+}$ [MnPy$_3$]$^{2+}$ +Me	17.10	17.10
[MnPy$_2$Me]$^{2+}$ [MnPy$_2$]$^{2+}$ +Me	28.45	27.68
[MnPyMe]$^{2+}$ [MnPy]$^{2+}$ +Me	45.24	44.87
[MnPy$_3$Me$_2$]$^{2+}$ → [MnPy$_3$]$^{2+}$+ 2Me	16.80	16.80
[MnPy$_2$Me$_2$]$^{2+}$ → [MnPy$_2$]$^{2+}$+ 2Me	71.44	71.42

The average pyridine binding energy, calculated as one-quarter of the energy of the reaction [Mn(Pyridine)$_4$]$^{2+}$→ Mn^{2+}+4Pyridine at the different levels of theory of zero point energy are in realistic agreement: BP86/6-311++G(d, p) 429.34 kJ mol-1; TPSSh/6-311++G(d, p) 429.5 kJ mol-1. The calculated binding energies equate to approximately 35,890 cm-1 per molecule, while at the same levels of theory the calculated one-third binding energy of the reaction [Mn(Pyridine)$_3$)$^{2+}$ → Mn^{2+}+ 3Pyridine at zero point energy corrections gave BP86/6-311++G (d, p) 519.32 kJ mol-1; TPSSh/6-311++ G(d, p) 519.32 kJ mol-1. This theoretical calculated binding energy corresponds to 43411.75 cm-1 per molecule. At optimised structure of [Mn(Pyridine)4]2+ the lowest energy structure was found to be a sextet state with a D4h symmetry, which was confirmed as an energy minimum by frequency analysis. All the N-Mn-N bond angles were found to be 90o and manganese nitrogen bonds were equidistance at 2.20 Å (Figure 5).
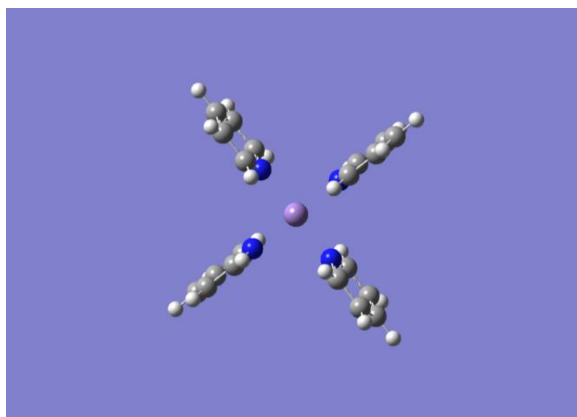

Figure 5. The optimised geometry of [Mn(Pyridine)$_4$ at BVP86, D$_4$h Symmetry

INTERACTION OF MANGANESE PYRIDINE DICATION ION WITH METHANE

When $[Mn(Pyridine)n]^{2+}$ interacts with the methane molecule the electron arrangement in the methane ligand is disturbed creating polarity on the methane. An electrostatic ion- induced dipole attraction between the metal coordinated unsaturated complex ion and the ligand plays a prominent role in the bonding. It has being observed that the binding of methane to a metal centre in a metal-coordinated unsaturated complex occurs in three different modes namely the η^1-, η^2-, or/and η^3-, where ηn designates nC−H bond interactions with the metal centre [9]. The binding mode of methane to the metal dication complex ion is determined by the M−C distance. In the optimised geometry the methane molecule possesses partial charges. Taking $Mn(Pyridine)_2]^{2+}$ binding with methane for instance, Gavin et al [9] observed that the absence of the η1-binding mode in the gas phase manganese cluster dicationic complex was due to repulsive interaction of the partial charge on the hydrogen atom with the positive charge at the metal centre. However, in both the neutral gas-phase and condensed-phase chemistry this effect is much less pronounce due to the fact that charges are highly delocalized. The repulsion is reduced in the η2- and η3-structures, primarily due to the fact that the positive charge of the metal ion can get much closer to the partial negative charge at the carbon atom of the methane molecule [9] by electrostatic interaction. At the fully optimised geometry of $[Mn(Pyridine)_4CH_4]^{2+}$ the manganese - methane (Mn-C) distance between the metal ion and the methane molecule is 1.90 Å. The hydrogen-carbon-hydrogen (H-C-H) angles in methane were distorted to between 108.65 and 110.40o, distorting the initial tetrahedral geometry of the $[Mn(Pyridine)_4]^{2+}$.

One Dimentional Potential Energy Curve Model Mn(PYRIDINE)$_4$(CH$_4$)]$^{2+}$
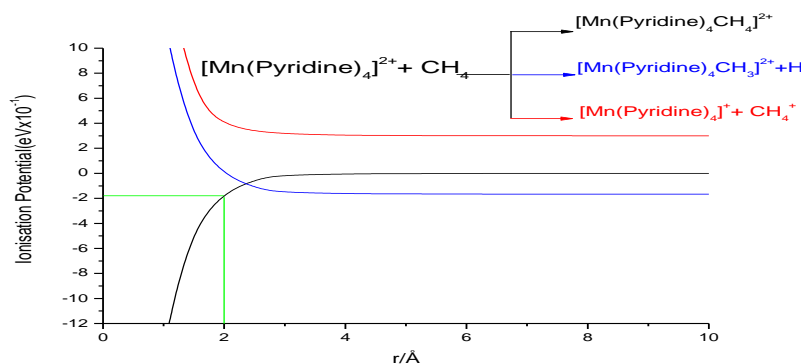

Figure 6. The potential energy surface curve model showing attractive curve of ion-ligand, H loss and repulsive curve

The photo-induced charge separation can be interpreted by the one dimensional potential energy curve model. The attractive curve captures and takes the ion-dipole and ion-induced dipole interactions between the metal ion and the ligand into consideration. Normally, the attractive force depends on the dipole moments and the polarisability of the ligand as a function of distance r between the metal ion and ligand. The extent of metal ligation on the methane binding energy has been investigated for $[M(Pyridine)_4(CH_4)]^{2+}$. As a way of demonstrating and visualising the observed charge separation reaction between the metal complex dication ion and the methane ligand, a one dimension PEC model has been plotted (Figure 6).

The minimum distance between the metal ion and the methane where the $[Mn(Pyridine)_4CH_4]^{2+}$ geometry is fully optimised was approximately r=1.90 Å. For the metal-methane carbon distance (Mn-C) where this occurs on the

potential energy curve is important, because it helps to determine the binding energy of the methane to the metal ligand dication complex ion. It is very crucial to maximize the methane binding energy as this decreases the energy barrier for oxidative insertion as binding energy increases [24] and this condition can be attained if the geometry is fully optimised. It is not surprising that the photo fragmentation yielded no charge transfer between the metal dication complex ion and the methane. This purely suggests that the electron affinity of the complex is lower than the ionization energy of methane. When such a condition is fulfilled in the ion trap; the possibility of charge transfer occurring is drastically reduced. The main advantage for such a condition is that it prevents any interesting side reactions from occurring in the ion trap [25].

The positions of these curves give a clear idea about the exothermicity of the reactions they correspond to at infinite separation. From the curves, it could be observed that the H transfer separation giving [Mn $(Pyridine)_4CH_3]^{2+}$+H from [Mn(Pyridine)$_4CH_4]^{2+}$ is located closer to the stable curve. When two reactants in a cluster move outward along the potential curve they will first experience an encounter at a shorter reaction distance hence the thermal collision between Mn^{2+} and CH_4 will encounter the H charge transfer curve before meeting the bond breaking curve. The photoinduced charge transfer to give [Mn(Pyridine)$_4]^+$ and CH_4^+ of [Mn(Pyridine)$_4CH_4]^{2+}$ was not observed because this reaction is endothermic as evidenced by observing that the PEC (red) lies above the attractive curve.

CONCLUSION

The calculated average pyridine binding energy at the different levels of theory of zero point energy are in perfect agreement which precisely falls within the experimental photon energy range over which the photofragmentation spectra were recorded. The binding energies of methane decrease drastically with increasing number of pyridine ligands in the order of [Mn(Pyridine)CH$_4]^{2+}$ > [Mn(Pyridine)$_2CH_4]^{2+}$ > [Mn(Pyridine)$_3CH_4]^{2+}$ > [Mn(Pyridine)$_4CH_4]^{2+}$. This behaviour is not unexpected since pyridine as a very effective Lewis base reduces the charge at the metal centre of the co-ordinately unsaturated manganese dication complexes. This consequently reduces the effectiveness of the metal−CH$_4$ electrostatic interactions.

The optimised structure of [Mn(Pyridine)$_4(CH_4)]^{2+}$ was observed to be of C1 symmetry and DFT calculation gave the binding energy of methane with the metal ion complex to be 15.13 kJ/mol while the optimised distance of approximately r=1.43Å.

The metal dication ion complex and the methane recorded the binding energy of 17.37 kJ/mol on the potential energy curve (PEC). This higher interaction energy extracted from the potential energy curve is due to the fact that the charge (Mn= 2) was assumed for the metal ion in the calculations for the PEC but at the optimised geometry the calculated actual charge on the metal ion is (Z=1.43 Å). Comparing the calculated DFT and PEC interaction energies for methane with manganese pyridine dication complex ion the electrostatic energy is drastically overestimated on the potential energy curve by 2.24 kJ/mol.

The calculated polarisability of methane is 2.470 Å3 which is in agreement with the calculated value of 2.472 Å3 obtained by Gavin et al [23] and with the experimental value of 2.448 Å3 [28]. An energy difference of less than 1 kJmol−1 in electrostatic calculation is observed when the calculated value and the experimental polarisability are applied. From this simple electrostatic investigation it is clear that methane contributed almost nothing to the reduction in charge at the metal center. The reduction in charge at the metal center may be purely due to the pyridine ligands which consequently reduce the binding energy of the methane with the coordinately unsaturated manganese dication complex ion.

REFERENCES

[1] J Felcher; U Schurath; R Xeliner. *Chem Unserer Zeit*. **2007,** 41,138
[2] PM Toriainen; X Chu; LD Schhmidt. *J Catal*. **1994,** 146, 1
[3] J Wei; E Iglesia. *J Catal*. **2004,** 224, 370
[4] AJ Stace. *J Phys Chem A* **2002,** 106, 7993.
[5] G Wu; D Chapman; AJ Stace. *Int J Mass Spectrom*. **2007,** 262, 211.
[6] M Mleczko; M. Bearns. *Fuel Process Technol*. **1995,** 42, 217.
[7] JH Lunsford. *Angew Chem Int Ed Engl*.**1995,** 34, 970.
[8] Wu Guohua; Stewart; Hamish; Lemon; Francis D; Cox; Hazel and Stace; Anthony. *J Mol Physics*. **2010,** 108: 7, 1199-1208.
[9] W Gavin; Roffe; Hazel Cox. *J Phys Chem A*. **2013,** 117.
[10]PM Torniainen; X Chu; LD Schmidt. *J Catal*.**1994,** 146, 1.
[11]F Besenbacher; I Chorkendoff; BS Clausen; B Hammer; AM Molenbroek; JK Nørskov; I Stensgaard. *Sci*.**1998,** 279, 1913.
[12]JP Van Hook. *Catal Rev Sci Eng*.**1980,** 21, 1.
[13]GF Froment. *J Mol Catal A*. **2000,** 163, 147.
[14]MC Bradford; MA Vannice. *Catal Rev Sci Eng*.**1999,** 41, 1.
[15]YH Hu; E Ruckenstein. *Adv Catal*. **2004,** 48, 297.
[16]AT Ashcroft; AK Cheetham; MLH Green PDF. *Vernon Nature*. **1991,** 352,225.
[17]MCJ Bradford; MA Vannice. *Appl Catal A*. **1996,** 142, 97.
[18]K Tomishige; YG Chen; K Fujimoto. *J Catal*.**1999,** 181, 91.
[19]ZL Zhang; XE Verykios. *Catal Today*. **1994,** 21, 589.
[20]M Pettre; C Eichner; M Perrin. *J Chem Soc Faraday Trans*. **1946,** 43, 335.
[21]D Dissanyake; MP Rosynek; KCC Kharas; JH Lunsford. *J Catal*.**1991,** 132, 117.
[22]DA Hickman; LD Schmidt. *Sci*. **1993,** 259, 343.
[23]VR Choudhary; AM Rajput; B Prabhakar. *J Catal*. **1993,** 139,326
[24]BE Bent. *Chem Rev*.**1996,** 96, 1361.
[25]WA Herrmann. *Angew Chem Int Ed Engl*.**1982,** 21, 117.
[26]P Biloen; WMH Sachtler. *Adv Catal*. **1981,** 30, 165.
[27]VF Fischer; H Tropsch. *Brennst Chem*.**1928,** 3, 39
[28]TV Choudhary; C Sivadinarayana; CC Chusuei; A Klinghoffer; DW Goodman. *J Catal*. **2001,** 199, 9.
[29]MG Poirier; C Sapundzhiev. *Int J Hydrogen Energy*. **1997,** 22,429.
[30]EK Lee; SY Lee; GY Han; BK Lee; TJ Lee; JH Jun; KJ Yoon. *Carbon*. **2004,** 42, 2641.
[31]GE Keller; MM Bhasin. *J Catal*.**1982,** 73, 9.
[32]PDF Vernon; MLH Green; AK Cheetham; AT Ashcroft. *Catal Today*.**1992,** 13, 417.